On Forecasting the Annual Cycle of Critical Ionosphere

Frequencies and Magnetic Storms

by G. M. Bartenev

ON FORECASTING THE ANNUAL CYCLE OF CRITICAL IONOSPHERE FREQUENCIES AND MAGNETIC STORMS

G. M. Bartenev

Presented by academician B. A. Vvedenskiy.

The numerous observations of the critical frequencies and the actual altitudes of the ionosphere during the course of the current 11-year cycle of solar activity make it possible to draw conclusions on the character of the variation in the ionization of the atmospheric layers during the course of the annual period. The ultimate object of this paper is to obtain computational formulae for forecasting the critical frequencies, as well as the number of magnetic storms, during which the quality of radio communication considerably deteriorates or is even completely interrupted.

Thanks to the large number of observations, it may now be considered as established that the ionization of the E and F_1 layers is primarily due to the ultraviolet rays of the sun, except in cases of abnormal sporadic ionization, which remains unchanged during the course of the night, when the influence of ultraviolet radiation is excluded.

According to Chapman's law [1], for a layer of the atmosphere ionized by monochromatic radiation of the sun, the critical frequency of the ionized layer at noon varies with the zenith angle of the sun in the following way:

$$f_{cr} = A \cos^{\frac{1}{4}} \theta$$

where A is a constant

- 1 -

This law satisfactorily describes the variations in the diurnal and seasonal ionization of the E and F_1 layers, but the behavior of the F_2 layer is not entirely subject to Chapman's law. This has been shown by ionosphere observations made at Huancayo, Peru [2], and also at Washington and Watheroo, Uoteru, published in the investigations of Berkner and Wells [3].

The ionization of the F_2 layer at noon in the northern hemisphere is less in midsummer than in winter, in December, when according to the law $cos^{\frac{1}{4}} \theta$ the ionization in June should be greater, since the zenith angle of the sun is less at this time.

In midsummer the density of ionization in the F_2 layer is lower at noon than at 1000 hours, and there is a second maximum at 1800 to 2000 hours. Thus instead of a single noon maximum there are 2 maxima; this indicates that more than a single cause is responsible for the ionization of the F_2 layer.

Before the session of the International Scientific Radio Union in September, 1934, Appleton suggested that the cause of this anomaly might be found in the considerable variation in the molecular temperature of the higher layers of the ionosphere. In consequence of the low molecular density of the air at the altitude of the F_2 layer, a considerable heating of the medium by the solar radiation may be assumed.

Appleton and Naismith [4] suggest that as a result of this heating, the altitude of the uniform atmosphere H is increased, since

$$H = \frac{kT}{mg}$$

where T is the absolute molecular temperature, k is Boltzmann's constant, m is the mean molecular mass, and g the acceleration of gravity.

This reduces the density ρ in the region where maximum ionization takes place, since according to Chapman

$$\rho = \frac{\cos x}{A H} \qquad (3)$$

where A is the absorption coefficient of radiation, x is the zenith distance of the sun, determined by the expression

$$\cos x = \sin \delta \cos \theta + \cos \delta \sin \theta \cos \Phi \qquad (4)$$

δ is the worth declination of the sun, θ is the zenith angle, Φ is the local time after noon, expressed in radians αt_{sec} or the longitude of the point, measured towards the east from the noon meridian at the moment of time t (time in seconds) that is

$$t = \frac{86,400 \, \Phi}{2 \pi} = 1.37 \cdot 10^4 \Phi \qquad (5)$$

whence

$$\Phi = 0.73 \cdot 10^{-4} t,$$

The reduction in ρ the density of the atmosphere, produced by the heating, reduces the maximum electron density N_{max}, since the full ionization attained at each definite level is now distributed over a greater thickness H of the ionized layer in question. [5]

- 3 -

The reduction in the noon ionization in midsummer is attributed by Appleton and Naismith to this circumstance [5].

Simultaneous and coordinated studies of ionization in the northern hemisphere (Washington, $\varphi \approx 39^\circ$ N) and the southern hemisphere (Watheroo, $\varphi \approx 30^\circ$ S), conducted by Berkner and Wells [4], demonstrated the untenability of the hypothesis seeking to explain the summer behavior of ionization in the F_2 layer by the heating of the ionosphere.

According to the observations at Washington and Watheroo, located almost symmetrically with respect to the equator, no summer effect on ionization of the F_2 layer is observed. The summer effect in the northern hemisphere proves to be general and simultaneous throughout the entire earth, and is thus observed in the southern hemisphere in winter, when the possibility of applying the heating hypothesis is excluded.

Moreover, according to the theory of Appleton and Naismith, the ratio of summer ionization density N_s to that in winter N_w is equal to

$$\frac{N_s}{N_w} = \left[\frac{\sin(\theta + \delta)}{\sin(\theta - \delta)} \left(\frac{T_w}{T_s} \right)^{\frac{1}{2}} \right]^{\frac{1}{2}} \tag{6}$$

Here T_w and T_s are the winter and summer molecular temperatures, taken as proportional to the electron temperature. On applying this expression to the Washington observations, we obtain a ratio of the summer molecular temperature to the winter, i.e. $\dfrac{T_s}{T_w}$, equal to 300, while according to the Watheroo observations this ratio is 2. Thus the temperature in the ionosphere over Washington

- 4 -

would be roughly 150 times higher than in the ionosphere over Watheroo, which is improbable.

The ionosphere observations at Washington and Watheroo, conducted by Berkner and Wells from 1933 to 1937 make it possible to reach the conclusion that there is an additional ionizing component, of period equal to one year, with a December maximum, and moving in phase for both hemispheres of the earth. This component has so great an amplitude that the seasonal variations in the ionosphere are completely masked.
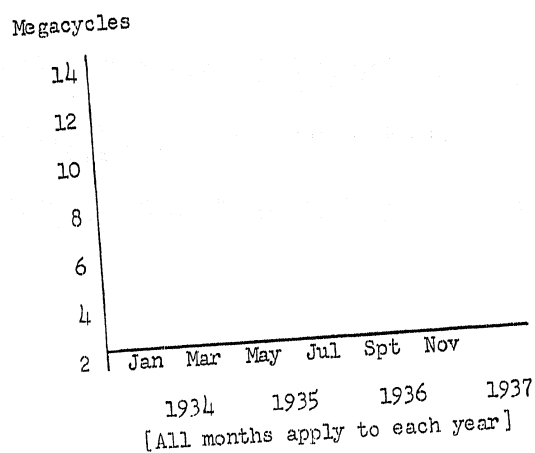
Megacycles

[All months apply to each year]

Figure 1

On the basis of the same experimental material from 1934 to 1938, T. L. Eckersley [5] held the detailed analysis of the F_2 layer ionization curves conducted by Berkner and Wells, disassociating them into secular, annual and seasonal components, to be well-founded, and turned his attention to the circumstance that in winter there is not one maximum but two, which are appreciably advanced towards the equinoxes (Figure 1).

- 5 -

In the course of his own detailed analysis, Eckersley came to the conclusion that there is also a half-year period in the ionization of the F_2 layer, due to the existence of active zones on the sun (at the average latitude of $\pm 15^\circ$ at the time of the maximum) and to the fact that the sun's axis of rotation is inclined to the plane of the ecliptic. In consequence of this, the earth on its orbit passes on 5 March and 7 September through those sectors most subject to solar radiations, and, conversely, passes in June and December through those sectors of its orbit that are least subject to solar radiation.

The existence of more complete experimental data than those at the disposition of Berkner and Wells, and likewise of Eckersley and others, now allows development of the work commenced by them up to the limit at which it will be possible to obtain computational formulae for forecasting the optimum frequencies of radio communication.

If the results of the ionosphere observations made at Washington from 1933 to 1945 are represented on a diagram $f_{kp} = \varphi(t)$, we obtain the curves shown on Figure 2. This figure shows the behavior of the critical frequencies for the E and F_2 layers, day and night, during the course of each month and year of the 11-year cycle; and in addition the flat curve characterizes the mean annual values of the critical frequencies f_E, $f_{F_2}^{-d}$, f_{F_2} and $f_{F_2}^{-M}$. As may be seen from the curve of noon values for the critical frequencies $f_{F_2}^{-d}$ of the F_2 layer, the peculiarities noted by Berkner and Wells, and likewise by Eckersley and others, in the behavior of the noon critical values are of systematic character throughout the entire 11-year cycle, which permits us to speak with great confidence of the
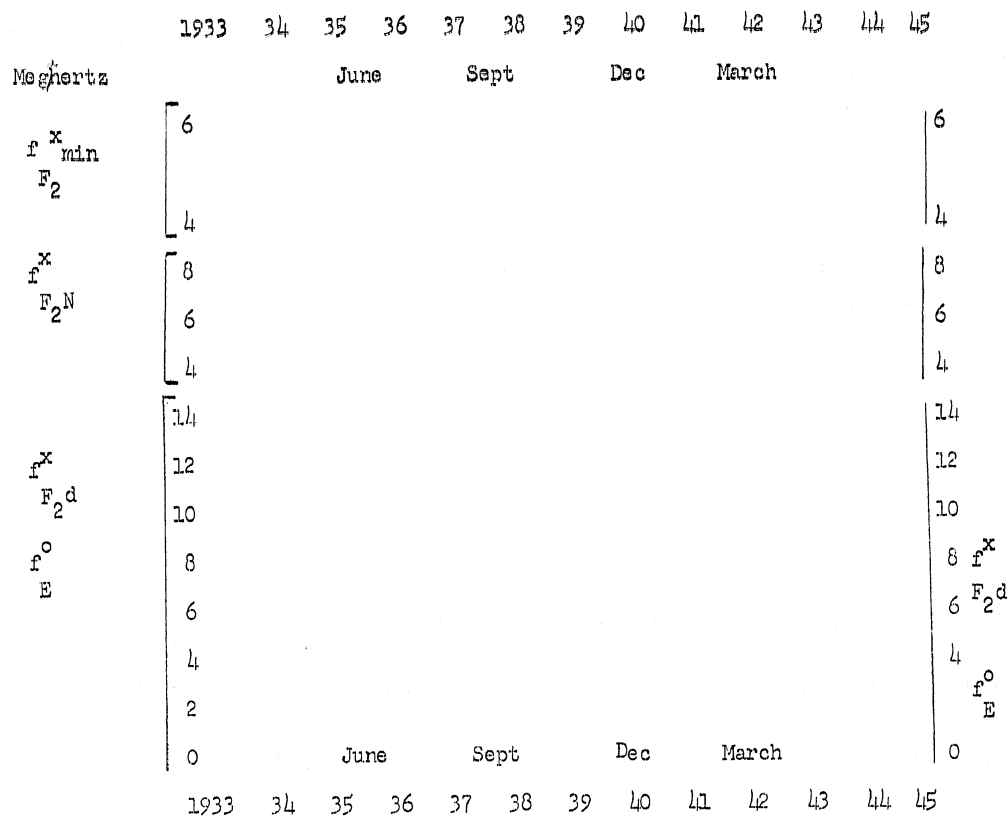
- 6 -

causes that produce variation in the march of the critical frequencies. Eckersley [5] has expressed the opinion that the causes producing these variations do not depend on the number of sunspots and have no connection whatever with any of the solar radiations. If the cause of the annual effect were the ultraviolet radiation of the sun, it would only be observed by day, but if it were due to causes not depending on the sun, and arising, for example, in stellar radiation, then the maximum effect would obviously be determined not by solar time but by sidereal time. Thus besides the noon maximum in December and January - for the northern hemisphere - there should also be a nocturnal maximum in June and July.

[See Figures 2 and 3 on next page]

Eckersley confirmed this opinion of his by the observations of the march of nocturnal ionization of the F_2 layer made at Tokio and published in the paper of Maeda, Tukada and Kamochida [6] (Figure 3).
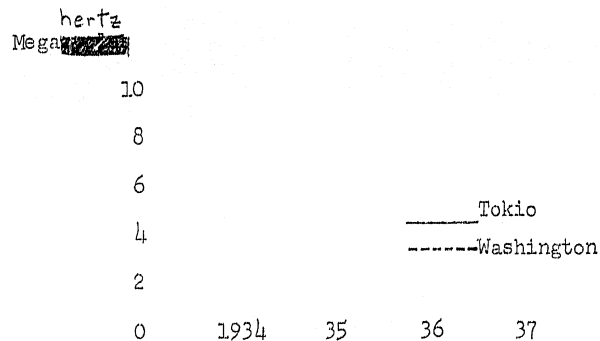
The observations of the Japanese were quantitatively inadequate to dispose definitely of the discussion provoked by Eckersley's hypothesis of the galactic origin of the ionization component responsible for the annual cycle.

The results of the observations of the critical frequencies $f_{F_2}^N$ of the F_2 layer at night, and of the minimum critical frequencies $f_{F_2}^M$ in the early morning hours at Washington, as shown on the top of Figure 2, confirm Eckersley's hypothesis, since the maximum ionization effect in these layers on a summer night represents a regular phenomenon over the course of every 11-year cycle.

Megahertz

1933 34 35 36 37 38 39 40 41 42 43 44 45

June   Sept   Dec   March

f^x_{min} F_2

6

4

6

4

$f^x_{F_2N}$

8

6

4

8

6

4

$f^x_{F_2d}$

f^o_E

14

12

10

8

6

4

2

0

14

12

10

8 f^x

6 F_2d

4

f^o_E

June   Sept   Dec   March

1933 34 35 36 37 38 39 40 41 42 43 44 45

[All months at top and bottom

apply to each year]

Figure 2

hertz

Mega▓▓▓▓

10

8

6

4   _____ Tokio

2   ------Washington

0   1934   35   36   37

[All months apply to each year]

Figure 3

- 8 -

This phenomenon may be even more sharply emphasized by representing in polar coordinates the observations shown in Figure 2, as we have done in Figure 4, and then, after calculating the monthly means for the noon night and minimum critical frequencies, for the year, over the entire 11-year cycle, also representing them in polar coordinates. (Figure 5).
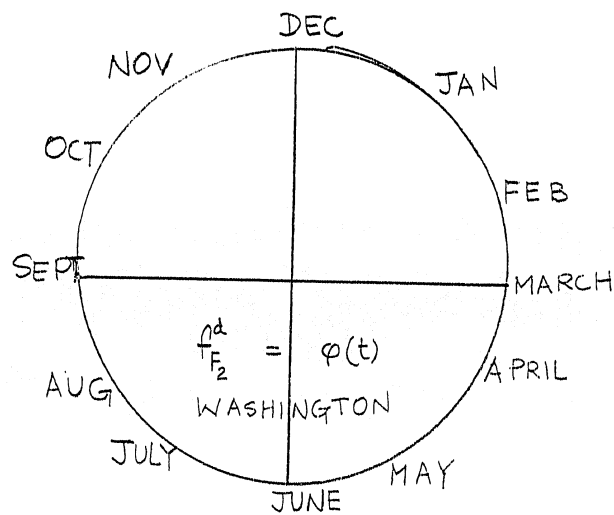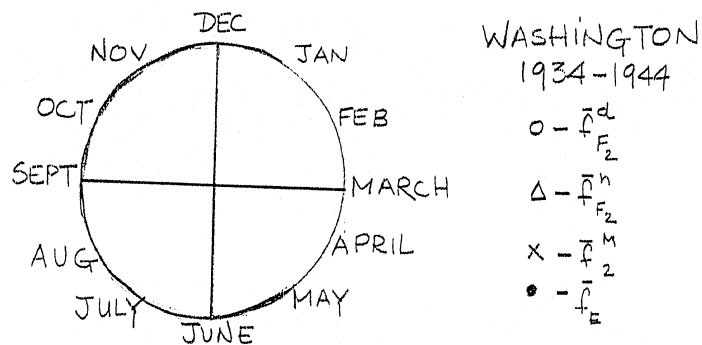

Figure 4

Figure 5

- 9 -

This comparative diagram of the general annual march of the critical frequencies, on which the maximum effect has been taken as unity, vividly emphasizes that the annual-march component, which has a single maximum in December-January, is due to radiation of non-solar origin, since it depends on the march of sidereal time.

Eckersley [5] has suggested that the amplitude of the annual-fluctuation component of the ionization should be equal to the difference between the summer and winter ionization minima. Having available experimental material only for the first half of the solar cycle, he found, on eliminating the component of seasonal fluctuation, that the mean value of this amplitude was ± 20 per cent of the level of the mean annual value of the secular (11 year) march in the variation of atmospheric ionization.

Since we now disposal (have at our) more complete material, covering the whole cycle, (Figure 5), we can now proceed to draw the same conclusion on the magnitude of the mean amplitude of the annual component, in the fluctuation.

Thus one of the components of the general curve (Figure 5) of the annual march $f^{-d}_{F_2} \varphi = (t)$ is a curve that does not depend on the 11-year cycle of sunspot variation, with an amplitude ± 20 per cent of the level of that secular cycle. Eckersley assumed this curve to be an ordinary sine-curve, but this is not entirely correct.

Assuming that, the annual variation in the critical frequencies is dependent, as Eckersley claims, on galactic radiation, that the orbit of the earth is a true circle and that the stream of galactic radiation falling on the edge of the earth's orbit represents a parallel pencil, we determine the character of the variation in the noon

critical frequency for the F_2 layer of the atmosphere during the course of the annual period, as the path of a point on a circle of contracted radius, intimately connected with the earth's orbit and rolling, without sliding along a line of constant intensity of galactic radiation. This line of constant intensity we take for the axis of abscissae and plot on it the time by months of the year,

(Figure 6). Here the circle of radius r_1, represents the orbit of the earth. If this circle rolled along the axis of abscissae without sliding, we would obtain an ordinary cycloid. But, if we limit the annual summer-winter fluctuation in the ionization of the F_2 layer by day, to ± 20 per cent which corresponds to the actually observed fluctuations in the critical frequencies, it is necessary to consider the rolling of a circle with the smaller radius r_2; this circle is intimately linked with the above-mentioned circle (the orbit of the earth). The locus of a point lying on the circumference of this smaller circle with radius r_2 as the circle rolls without sliding, represents a contracted cycloid, or what is termed a trochoid, rather than a since curve, as Eckersley assumed in first approximation.

Taking as parameter the angle QOP = φ, which corresponds on the axis of abscissae to the segment traversed by the earth during its rolling along the orbit, we find how the ordinate QR, which is proportional to the value of the frequency $f_{F_2}^{-d}$, varies during the course of a year.

It is clear from Figure 6 that

$$f_{F_2}^{-d} = QR = OP - ON$$

But since

$$OP = r_1,$$

$$ON = r_2 \cos \varphi,$$

then

$$\bar{f}_{F_2}^{d} = QR = r_1 - r_2 \cos \varphi,$$

- 11 -

where φ is an angle proportional to the season of the year.

We find the numerical expressions for r_1 and r_2 on the basis of experimental data.

Berkner and Wells [4], and also Eckersley [5], have estimated in detail the various components of the annual march at atmospheric ionization. According to Eckersley the amplitude of the component of annual fluctuation amounts to ± 20 per cent. This figure remains true, on the average, throughout the entire cycle. Thus the radius of the smaller circle r_2 will be equal to 0.2.
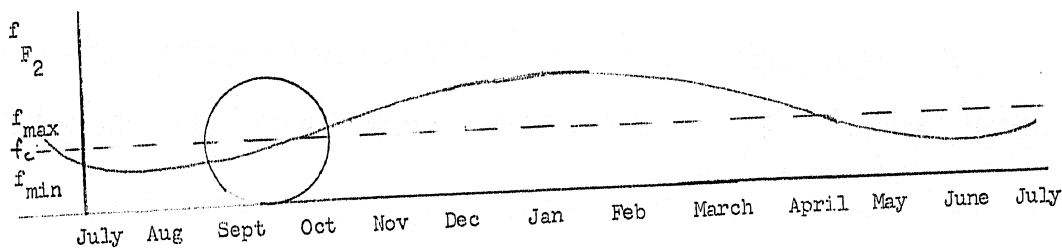

Figure 6

The value of r_1 is equal to the ordinate of the small circle (Figure 6), if it is taken as constant throughout the year. The component of annual fluctuation r_2 will vary during the course of the 11-year cycle as shown on Figure 7.

In fact, the component r_1 is not constant throughout the 11-

year (secular) cycle, and varies proportionately to the variation
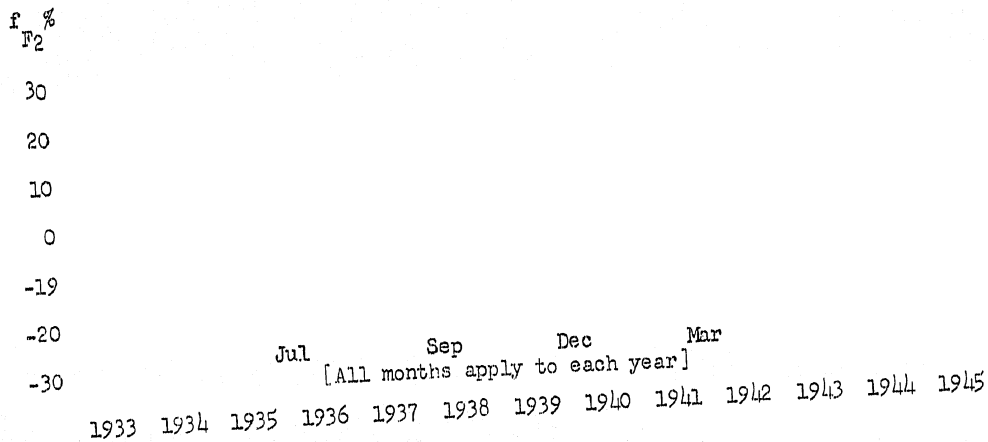
in the mean annual value of the critical frequencies.

f_{F_2} %

30

20

10

0

-19

-20

-30

Jul   Sep   Dec   Mar
[All months apply to each year]

1933 1934 1935 1936 1937 1938 1939 1940 1941 1942 1943 1944 1945

Figure 7

The value of r_1 thus corresponds to the critical frequency

of the secular march, i. e.

$$r_1 = \overline{f}^d_{F_2} \quad \text{secular}$$

Substituting now for the angle φ its value for each month,

of the year, i. e.

$$\varphi^\circ = \frac{2\pi}{12} t = (30t)^\circ$$

(where $t = 1, 2, \ldots, 12$),

we shall have instead of (7):

- 13 -

$$\bar{f}^{d}_{F_2 \Gamma} = \bar{f}^{d}_{F_2 \text{ SECULAR}} - 0.2 \cos(30t)^{\circ}, \tag{8}$$

where $t = 1, 2, \ldots, 12$ corresponds to January, February, etc. to December.

We now proceed to the determination of the semiannual component. The second principal component that enters into the general annual cycle of variation in the ionization of the atmosphere is the semiannual component.

If we consider from year to year the spiral curve shown on Figure 4, we shall note that as the 11-year cycle of ionization develops, the individual curves for each year, which at first are of epicycloidal character, change their form, and become deformed during the winter months (December to January), thanks to which cusps are formed at the time of the autumn and spring equinoxes. As the rate of solar activity falls, the annual curves again resume their original shape. This deformation of the epicycloids, which reaches its greatest extent during the time of maximum solar acti - vity, is shown on Figure 8. The observations in Washington and Tomsk in 1937 and in Bukhta Tikhaya in 1939 [7] (Figure 8) clearly illustrate these points.

o - Washington
△ - Tomsk
● - Bukhta Tikhaya

Figure 8
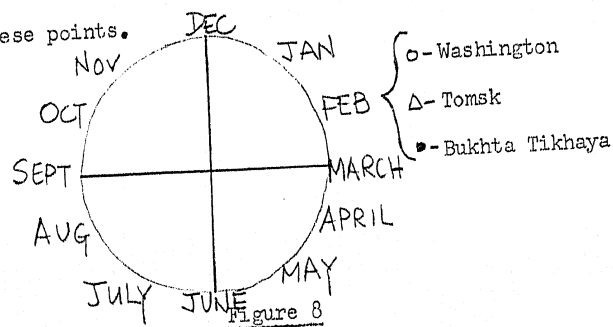
In addition to this, study of the catalog of magnetic storms according to the data of the Slutsk observatory of the period from 1878 to 1914 enables us to reach the conclusion that there is a sharply expressed semiannual march of the number N of magnetic storms, with spring and fall maxima (cf. table of distribution of the number of magnetic storms by months).

[See Table on following page]

Figure 9 is a polar diagram of the distribution of the number of geomagnetic storms, by months, for the period from 1878 to 1914. The radius-vector of this diagram is the number of magnetic storms taking place in the given month during the period from 1878 to 1914, while the argument is the time of year.

Figure 9
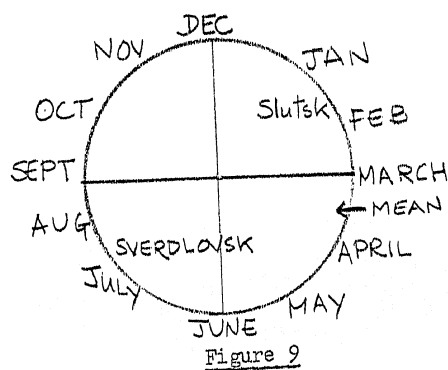
The construction of this diagram confirms the existence of a semiannual wave in the curves of geomagnetic activity as well. This phenomenon, known by the term Corti effect, subsequently termed Corti-

TABLE OF DISTRIBUTION OF THE NUMBER OF MAGNETIC STORMS BY MONTHS

	JAN	FEB	MAR	APR	MAY	JUN	JUL	AUG	SEPT	OCT	NOV	DEC
Number of Magnetic Storms	61	81	86	68	65	49	52	63	73	72	65	48
Number of Magnetic Storms Related to Spring Maximum	0.71	0.94	1	0.79	0.755	0.57	0.605	0.73	0.85	0.838	0.755	0.56

Felitsyn effect (after Felitsyn [8] refuted the doubts of Yu. Bartels as the existence of the effect), arises in consequence of the fact that the geographic latitude (breadth) of the earth's equator does not coincide with the latitude of the sun's equator as we have already pointed out.

The diagram of magnetic-storm statistics (Figure 9) indicates to the same extent the existence of a definite zonal character in the active areas on the sun, to the same extent as on the diagrams of atmospheric ionization, and confirms the view that the direction of the stream of solar corpuscular radiation which produces geomagnetic storms, is primarily normal to the surface of the sun and has a small solid angle, which according to the investigations of M. N. Gnevishew and A. I. Ol, is equal to 8 or 9°.

On the lines of radio communication studied in 1944 according to the operating data of a number of radio lines, the semiannual march of geomagnetic disturbance in the ionosphere is likewise strongly reflected, as is well shown in Figure 10. The curves characterize the operation of the main radio lines under investigation during the day when the magnetic characteristic is equal to

$$M = 0, \qquad M = 0.5, \qquad M > 1.$$

MONTHS

Figure 10

- 17 -
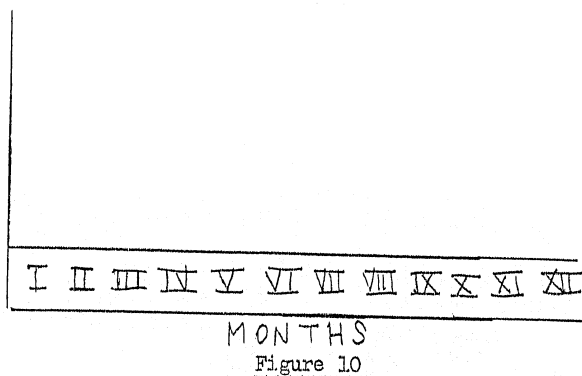
The time, by months in 1944, is laid off along the axis of abscissae, and along the ordinates is plotted an expression, in percent, of communication interrupted equal to

$$K\% = \frac{t - t'}{t} \times 100, \tag{9}$$

where t is the scheduled operating time, and t' is the actual time operated.

These points may be even more clearly illustrated if the curve M=0 (Figure 10) is taken out of the curve for M $>$ 1 and the curve IV so obtained is plotted on the diagram of Figure 9 (curve K). Here, by means of substracting the ordinate of the curve M=0 from the ordinates of the curve M $>$ 1, we eliminate the influence of the various factors that interfere with radio communication, other than the influence of magnetic disturbances in the ionosphere.

The predominance, in all seasons, of the geoactive indices of solar activity in the corresponding hemisphere of the sun (which results in the inequality of the ordinates of autumn and spring maxima) has been pointed out by Felitsyn [8] on the basis of a study of the march of the prominences. We see the same thing in Figure 9 with respect to the number N of magnetic storms as well. The spring wave of magnetic storms according to the Slutsk catalogue is dominant over the autumn wave. The march of the magnetic storms according to the Sverdlovsk catalogue is shown by dotted lines on Figure 9 as the mean value of the number N of magnetic storms during the four cycles from 1901 to 1945. The continuous thin line shows the mean value of magnetic storms according to the Slutsk catalogue.

- 18 -

Christy and Carrington [10] first directed attention to the zonal character of the active zones on the surface of the sun, which produce the semiannual wave in the march of atmospheric ionization (Figure 8) and in the march N of the number of magnetic storms (Figure 9). Subsequently Sporer [11] established his law of the movement of the active zones during the 11-year cycle. The accumulation of new data after the investigations of these astronomers now makes it possible to construct a diagram (Figure 11), on which the march of
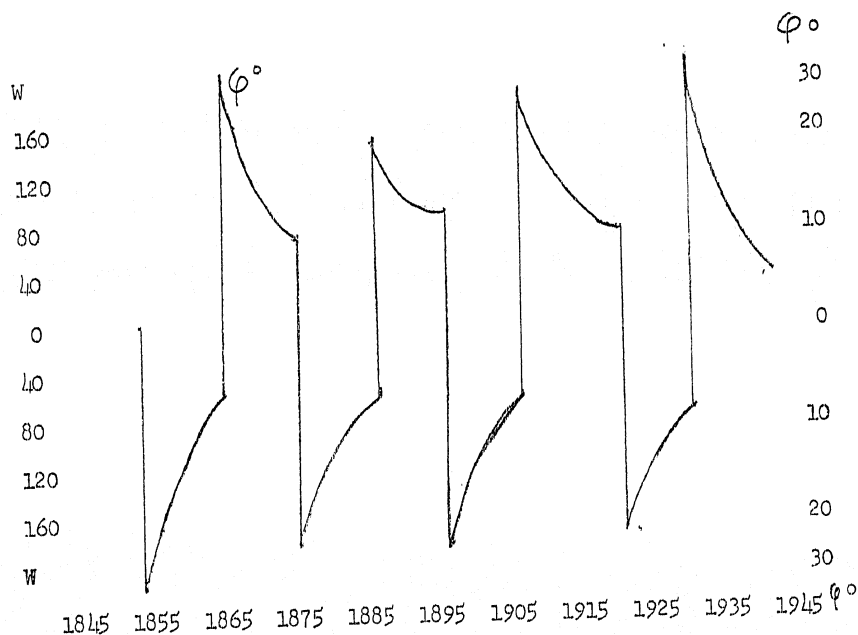
Figure 11

the active zones on the surface of the sun are shown, for the 8 cycles from 1855 to 1945 by their direction from the high solar latitudes phi φ ° towards the equator, together with the variations in the Wolf numbers W. This diagram gives a clear idea of the facts that

the active regions on the surface of the sun are principally located
between 5 and 30° of north and south latitude: and the maximum num-
ber of active zones of sunspot formation, on the average, corresponds
to latitude 15°, varying in accordance with the intensity of the cycle,
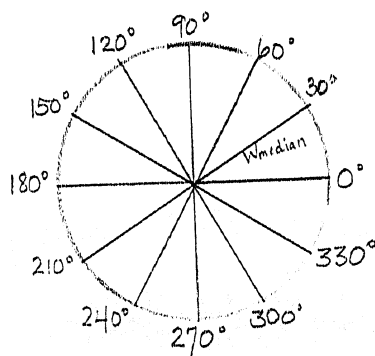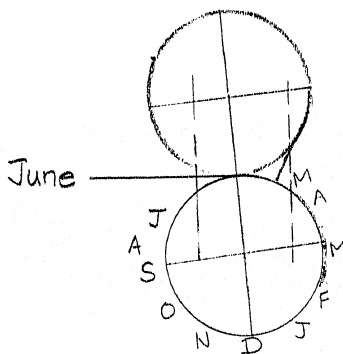within the limits of 11 to 18° south and north solar latitude [12].

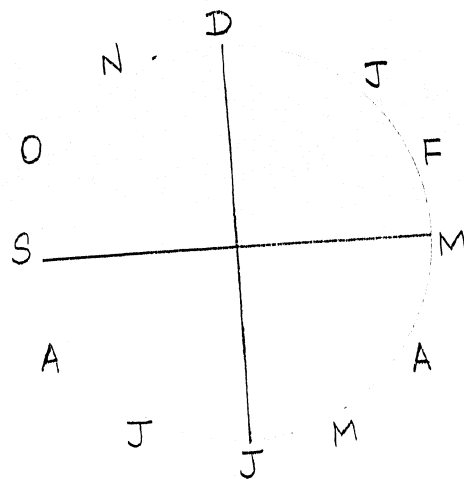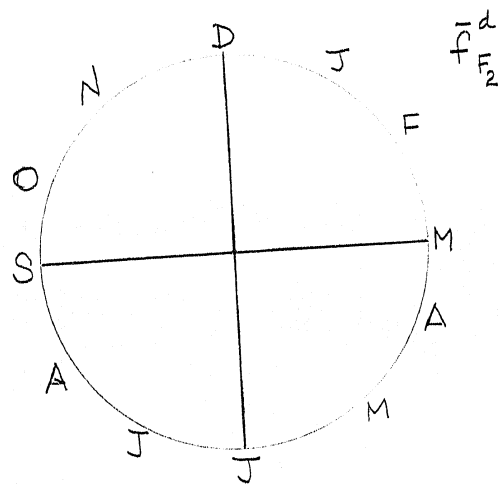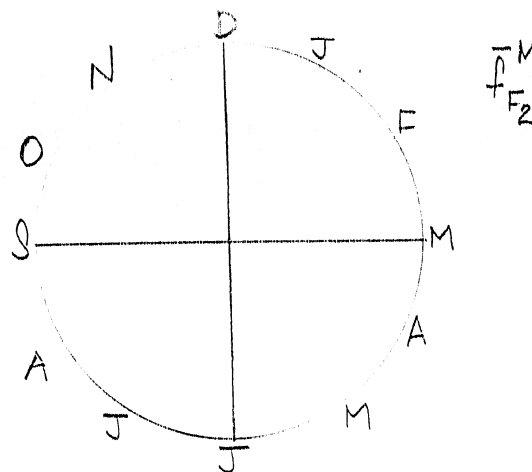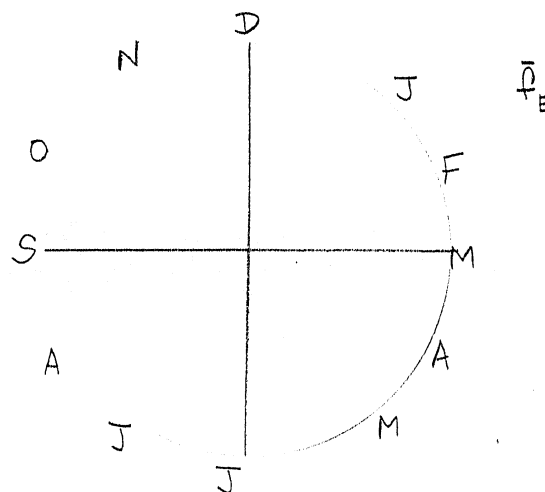Figure 12

Figure 13

Figure 14

Figure 15

Figure 16

Figure 17

To give a graphic representation of the picture of variation in the intensity of solar activity throughout the 11-year cycle, the dependence of "W" on φ^o (solar latitude) is shown in polar coordinates on Figure 12, for the minimum, mean and maximum intensity of the cycle.

The curve $W = f(\varphi^o)$ (Figure 12) may be generalized by an enveloping curve, known by the term "rose", expressed as follows in polar coordinates:

$$\rho = \rho_o \sin(n\varphi) \qquad (10)$$

where ρ is the radius-vector, varying from $-\rho$ to $+\rho$ as $n\varphi$ varies from 0 to 360 degrees.

Expression (10) may be transformed into a formula serving to forecast the Wolf numbers [1] [(1) See the author's dissertation "On the forecasting of radio communications".)], as follows:

$$W = W_o \sin^m 6\varphi, \qquad (11)$$

where

$$m = p_o + p_1 t + p_2 t^2 + \dots + p_m t^n$$

Here t is the time by year of the cycle, and P_0, P_1, P_2 are constants determined for each individual cycle.

Thus, considering as we do that the existence on the sun of zones of maximum activity emitting a more or less directional radiation is indisputable, it is possible for us to propose the following method of forecasting the semiannual component in atmospheric ionization and the semiannual march of geomagnetic disturbance and disruption of radio communication.

23

The diagram of the 11-year march of radiation from the active zones, as shown on Figure 12, is represented by the congruent petals of a rose. In consequence of the symmetry of the radiation with respect to the axes of rotation of the Sun, the petals of the rose form a figure of rotation, the maximum radiation (radius-vector) of which is oriented, on the average, towards the angle = 15 degrees of south and north solar latitude. This radius-vector, which symbolizes the magnitude and direction of the radiation, coincides with the normal to the solar surface at those places which most actively emit corpuscular and ultraviolet radiation during the epoch of maximum activity (Figure 13).

The sun's axis of rotation is inclined to the plane of the ecliptic at an angle of 7.2 degrees. The figure of rotation of the rose around the sun's axis, subjected to section at this angle, may be taken in its lowest part as the paraboloid of rotation with axis z, expressed by the following equation:

$$\frac{x^2}{P} + \frac{y^2}{P} - 2z = 0. \tag{12}$$

The equation of the plane so cutting the paraboloid of rotation at the angle of 7.2 degrees, and passing through the origin of coordinates, is:

$$-x \cos \alpha + z \cos \gamma = 0 \tag{12'}$$

This plane is located in such a way that a line lying upon it and coinciding with the diameter of the ecliptic is located along the y axis perpendicular to the plane of the upper part of the drawing (Figure 13).

Equations (12) and (12') yield

$$y^2 = x\left(2p\,\frac{\cos\alpha}{\cos\gamma} - x\right). \qquad (13)$$

This is the equation of a circle with the origin of coordinates lying on it, and the radius of which is determined by the expression

$$r = p\,\frac{\cos\alpha}{\cos\gamma}$$

and is located along the x axis.

In polar coordinates expression (13) takes the following form:

$$\rho = 2r\,\cos\psi. \qquad (14)$$

The curve presented on the lower part of Figure 13 is a section of the northern and southern paraboloids of rotation and is a lemniscatoid with the following equation:

$$\rho^2 = 4r^2\cos 2\psi$$

This curve belongs to what is termed the class of sinusoidal spirals, for which the general expression is of the form

$$\rho^m = 2r^m\,\frac{\sin}{\cos}(m\psi).$$

If we compare the curves that characterize the march of the critical frequencies at their maxima (Figure 4), and the values of the march of the number of magnetic storms obtained as the mean of the data of the Slutsk and Sverdlovsk catalogs (Figure 9, curve marked "mean") with the curve in Figure 13 (lower part), which is expressed by Equation (15), by superimposing the curves on the same chart (Figure 14), we see that equation (15) does not accurately characterize the distribution of magnetic storms.

For $\psi = 90$ degrees or $\psi = 270$ degrees, ρ will be zero by Equation (15), while on the diagram (cf. Figure 9) we have a value for ρ, at these angles, which is not less than 0.56 of the maximum December value of N and not less than 0.57 of the maximum June critical frequencies.

On the diagram of Figure 14, besides the lemniscatoid and the distribution curve for the magnetic storms, curves belonging to the same class of sinusoidal spirals are also plotted -- Cassini ovals. On comparing the surve of distribution of storms with these ovals it is clear that the distribution of storms (denoted by dots) can be well expressed by the equation of the Cassini oval, which represents the locus of points separated from two given points F_1 and F_2 by a constant distance τ^2, equal to the product of the distance of these two points to the point sought on the Cassini oval. These given points F_1 and F_2 are separated from each other by the distance 2r.

Since (by Figure 14)

$$\rho_1^2 = \rho^2 + r^2 - 2\rho r \cos\psi,$$
$$\rho_2^2 = \rho^2 + r^2 + 2\rho r \cos\psi,$$

then

$$\rho_1^2 \rho_2^2 = (\rho^2 + r^2)^2 - 4\rho^2 r^2 \cos^2\psi = \tau^4,$$
$$\rho^4 + r^4 + 2\rho^2 r^2 \cos^2 2\psi = \tau^4.$$

Whence we have, as the general equation of the Cassini ovals,

$$\rho = r \sqrt{\cos 2\psi \pm \sqrt{\cos^2 2\psi + \frac{\tau^4}{r^4} - 1}} \qquad (16)$$

The Cassini ovals corresponding to the three basic conditions

$$\tau > r, \quad \tau = r, \quad \tau < r$$

are plotted on Figure 14.

The first case -- curve I -- is expressed by Equation (16); the second case -- curve II -- is the Bernoulli lemniscate expressed by

$$\rho = r \sqrt{2 \cos \psi}$$

the third case -- curve III -- is expressed by the equation

$$\rho = r \sqrt{\cos 2\psi \pm \sqrt{\cos^2 2\psi - \cos^2 2\alpha}}$$

where $\dfrac{\tau^2}{r^2} = \sin 2\alpha$.

On this net of sinusoidal spirals (Figure 14), we plot the curve of the annual march of the mean values for the number of magnetic storms obtained by averaging the statistical data published in the Slutsk and Sverdlovsk catalogs of magnetic storms (Figure 9, curve of mean values).

Judging by the coincidence of the curve of magnetic storms indicated by dots on Figure 14, with curve I of the Cassini ovals, it may perhaps be considered that the annual march of magnetic storms is well described by Equation (16). But since we are only interested in the actual values, we shall have, instead of Equation (16)

27

$$\rho = r\sqrt{\cos 2\psi + \sqrt{\cos^2 2\psi + \beta}} \qquad (17)$$

where the parameter

$$\beta = \frac{\tau^4}{r^4} - 1 \qquad (A)$$

depends on the value of ψ, which is, on a certain scale, proportional to the secular march of N_W, the number of magnetic storms, which number is readily determined on the basis of the good correlation of N_W with the Wolf numbers W [1][(1) See other paper by the author in this journal.]

Thus instead of parameter (A) we may write

$$\beta = \frac{\tau^4}{N_W^4} - 1.$$

The value of

$$\tau^2 = \rho_1 \rho_2$$

within this parameter, is constant for the correct Cassini oval [Equation (17)]. The numerical expression for τ^2 may be determined by the method of quadratic approximation of periodic functions, using trigonometric polynomials.

Placing, for convenience, $\frac{\tau^2}{r^2}$ (Figure 14), or, what amounts to the same thing, $\frac{\tau^2}{N_W^2} = \sec 2\alpha$, we obtain, instead of the expression (17)

$$f(\psi) = \rho = N_W \sqrt{\cos 2\psi + \tau \sqrt{\frac{\cos^2 2\psi \cos^2 2\alpha}{N_W^4} - 2\cos^4\alpha}}$$

$$(18)$$

28

Since (18) is a real function and applies to all real axes $-\infty < \psi < +\infty$ and has the period 2π, we may start out, in order to approximate it, from the polynomials,

$$T_n(\psi) = a_o + \sum_{m=1}^{n} (a_m \cos m\psi + b_m \sin m\psi),$$

where the coefficients a_m and b_m are real numbers.

Regarding the function phi-psi $\varphi(\psi)$ given within the period ($-\pi \leq \psi \leq \pi$) as an integral weight, we set the task of reducing to a minimum the integral

$$\int_{-\pi}^{+\pi} [T_n(\psi) - f(\psi)]^2 d\varphi(\psi), \qquad (19)$$

which by Weierstrass's second theorem [13] approaches zero as n increases without limit.

In consequence of the fact that the functions

$$\gamma_o(\psi) = 1, \quad \gamma_1(\psi) = \cos(\psi), \quad \gamma_2(\psi) = \sin(\psi), \quad \gamma_3(\varphi) = \cos 2\varphi$$
$$\gamma_4(\psi) = \sin 2\psi$$

etc., form a linearly independent system, it becomes possible as the only method, to select a system of trigonometric polynomials, orthogonal within the period ($-\pi, +\pi$) with respect to the weight $\varphi(\psi)$.

By means of trigonometric polynomials of first, second and higher degree, the function $f(\psi)$ was aligned to the twelve successive ordinates corresponding to the months of the year, on the basis of which it was found that the value t has a mean value of 0.784 with an error not exceeding 7 percent.

On substituting the numerical value of t in the parameter β ▬ in Formula (17), and replacing the expression ρ by N_r

and r by $\overline{N}_W$, we finally obtain the following expression for fore-

casting the annual march of the number of magnetic storms

$$N_r = \overline{N}_W \sqrt{\cos 2\psi + \sqrt{\cos^2 2\psi + \frac{0.787^4}{\overline{N}_W^4} - 1}}, \quad (20)$$

where $\psi = (30t)^\circ$ ($t=1,2,3,\ldots\ldots,12$ -- the months of the year).

In deriving Equation (20), which defines the annual march of

magnetic storms, we confine ourselves to the only physically exist-

ing cause that disturbs the smooth secular march of magnetic storms

and is responsible for the spring and fall maxima.

But we have no right to limit ourselves similarly in study-

ing the annual march of atmospheric ionization. While in the case

of magnetic disturbances taking place as the result of non-station-

ary phenomena on the surface of the sun, such as the appearance and

disintegration of sunspots in the neighborhood of the central

meridian, we still could confine ourselves to the mere statisti-

cal number N of magnetic storms, it is necessary, in studying the

annual march of ionization, as we have already seen, to take account

of the continuously acting causes that produce variation in the to-

tal amount of ultraviolet and corpuscular radiation falling on the

earth.

It will be clear from the foregoing that in considering the

variation in the march of ionization during the course of a single

year, we may confine ourselves to three components. The annual

component, with a maximum in December-January, has the character

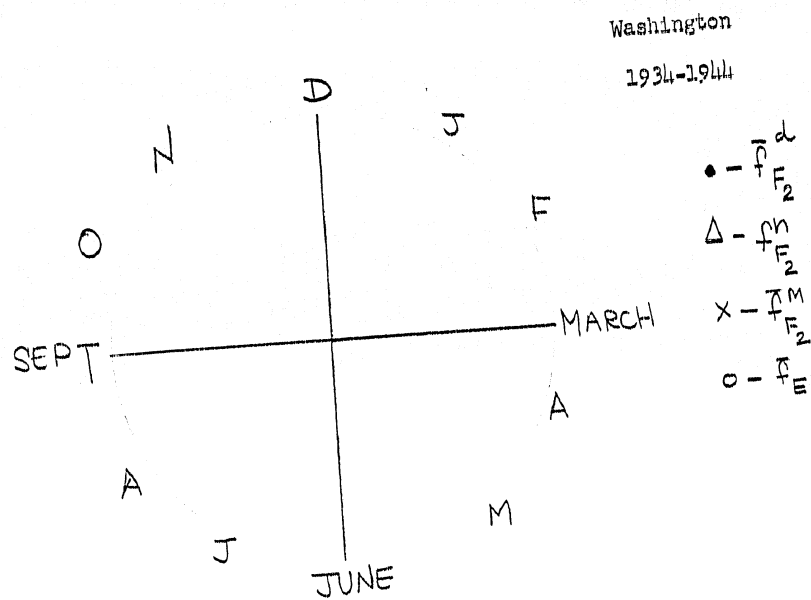of a trochoid. The semiannual components with maxima in spring and

Washington

1934-1944

$\bullet - \bar{f}^d_{F_2}$

$\Delta - f^h_{F_2}$

$\times - \bar{f}^M_{F_2}$

$o - \bar{f}_E$

D

N

J

O

F

SEPT ——————————— MARCH

A

A

M

J

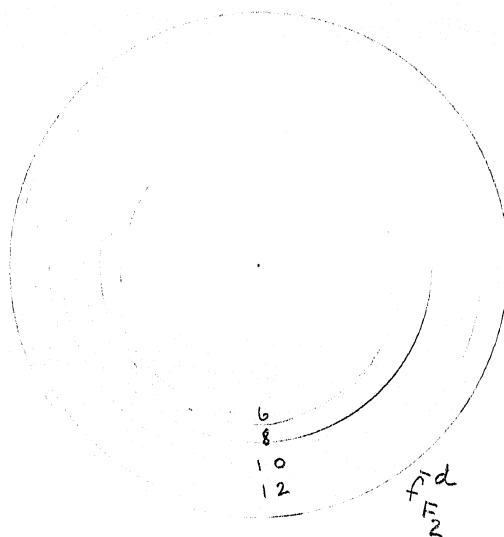JUNE

FIGURE 18

$f^d_{F_2}$

6

8

1 0

1 2

FIGURE 19

31

fall could be well represented by a Cassini oval, if it were not for the galactic corpuscular radiation postulated by Eccersley, which changes the shape of the ionization curve from a Cassini oval into an epicycloid, as may be seen from Figure 5, which represents the annual curves of the march of ionization of the layers of the ionosphere, averaged over the eleven years of the current cycle. Finally, the seasonal component, due to the inclination of the earth's axis to the plane of the ecliptic, has its maximum in June.

The curve of the seasonal march of ionization, as is clearly seen for the E layer (cf. Figure 5), can also be classified, in first approximation, as an epicycloid. For greater reliability in determining the character of the curves of the general annual march of the variation of ionization in the upper layers of the atmosphere, we have represented in megacycles (Figures 15, 16 and 17) the march of the critical frequencies by years of the 11-year cycle, at noon, for the F_2 layer (Figure 15), the march of the early morning minimum values -- half an hour before sunrise -- for the F_2 layer (Figure 16), and the march of the critical frequencies in the E layer at noon (Figure 17). To avoid complicating the picture, the whole 11-year cycle is not plotted on these diagrams. Each cycle, indicated by a spiral, corresponds to a single year.
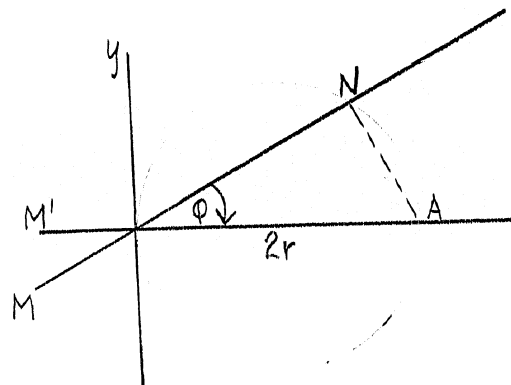
FIGURE 20

For the analytical determination of the shape of the curves in general form, we present in Figure 18 the mean values of the annual march of critical frequencies for 11 years for the F_2 layer (noon, midnight, and the minimum values) and for the E layer (noon values).

The curves thus obtained recall the cardioid, with its point of inflection for the curve $\overline{f}\, {}^{d}_{F_2} = \varphi(t)$ in June and for the other curves in December (Figure 18), but a cardioid may belong to any of three classes of curves, epicycloids, sinusoidal spirals, and "helices". The cardioid has a singular point at the origin of coordinates, which also constitutes a point of inflection. This cannot be said, however, of the critical-frequency curves we have derived (Figure 18), since the origin of coordinates in this case is the isolated point O.

33

$\bar{f}_{F_2}^{d} = \varphi(t)$ We shall first investigate only a single curve, namely
$\bar{f}_{F_2}^{d} = \varphi(t)$. This curve does not possess polar symmetry, inasmuch as the value of the critical frequency in December does not coincide with the value in June. But if the center be advanced to Point 2 (on Figure 19), then these values do coincide. We pass rays through the center O, joining the points of the curve derived, thus dividing each ray into the two equal parts $b_1 = b_2$ (Figure 19) and join the points that divide each ray. It then appears that the locus of these points represents a curve of almost circular shape and a diameter (O-2), equal to 2 megacycles (Figure 19). We now find that analytical expression of the values $\bar{f}_{F_2}^{d}$ which represents the radius-vector of the curve (19) in polar coordinates. For this purpose we represent separately, on an enlarged scale, the central part of Figure 19 (shown separately in Figure 20), where the circle of diameter 2r constitutes the above mentioned locus of the points dividing the rays in half.

We now determine the length of the radius-vector $f_{F_2}^{d} = OL$.

Since

$$OL = 2r \cos \varphi + b,$$

then

$$\bar{f}_{F_2}^{d} = 2r \cos \varphi + b. \tag{21}$$

The curve obtained represents the polar equation of Pascal's helix, with a center which is an isolated singular point, since $b >$ 2 r.

34

In order to maintain the location of the curves which we have adapted (Figures 18 and 19), when the axis of abscissae coincides with the spring and fall equinoxes, we transform expression (21) as follows:

$$\bar{f}_{F_2}^d = 2r \sin\varphi + b$$

Assuming, as in equation (8) that $\varphi = 30\tau = \frac{\pi}{6}t$, where t equals 1,2,3, ..., 12 for January, February etc., we shall finally obtain:

$$\bar{f}_{F_2}^d = 2r \sin\frac{\pi}{6}t + b$$

On making a similar study of the curves

$$\bar{f}_{F_2}^n = \varphi(t) , \quad \bar{f}_{F_2}^m = \varphi(t), \quad \bar{f}_E = \varphi(t),$$

we find that they are also well described by the equation of Pascal's helix with an isolated singular point, namely:

$$\bar{f}_{F_2}^n = 2r_1 \sin\frac{\pi}{6}t^o + b_1, \tag{23}$$

$$\bar{f}_{F_2}^m = 2r_2 \sin\frac{\pi}{6}t^o + b_2, \tag{24}$$

$$\bar{f}_E = 2r_3 \sin\frac{\pi}{6}t^o + b_3. \tag{25}$$

35

The numerical estimation of r, b, r_1, b_1, r_2, b_2, r_3, and b_3 in equations (22), (23), (24), and (25) for the 11-year summer mean of the annual cycle (from 1933 to 1944), may be carried out as follows.

On superimposing the radius-vector $\overline{f}_{F_2}^d = OL$ on the axis of abscissae, which is the line joining the points of the summer and winter solstices (Figure 20), we see that

$$b = AL' = \frac{OL' + OM'}{2}$$

On the other hand,

$$2r = OA = \frac{OL' - OM'}{2}.$$

On substituting for the segment OL' in these equations the value of $\overline{f}_{max}$ of the critical frequencies in the F_2 layer at noon (for the time of the December solstice), which is proportional to that segment, and substituting for the segment OM the value of $\overline{f}_{min}$, we have

$$b = \frac{\overline{f}_{max} + \overline{f}_{min}}{2}$$

(26)

$$2r = \frac{\overline{f}_{max} - \overline{f}_{min}}{2}$$

We obtain similar expressions b and $2r$ for the critical frequencies of the F_2 layer (night-time and early morning hours), and for the critical frequencies of the E layer, with the single difference that the maximum values for the frequencies of these layers will be in June, and the minimum values in December.

Using the mean values for the annual march of critical fre-
quencies observed at Washington, putting their maximum value as
unity, and applying expressions (26) and (27), we have

$$\bar{f}^{d}_{F_2} = 2 \sin \frac{\pi}{6} \tau + 9,$$

$$\bar{f}^{n}_{F_2} = 0.85 \sin \frac{\pi}{6} \tau + 4.92$$

$$\bar{f}^{m}_{F_2} = 0.375 \sin \frac{\pi}{6} \tau + 4.325$$

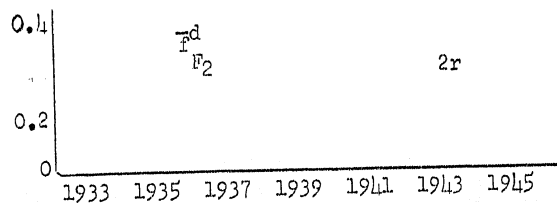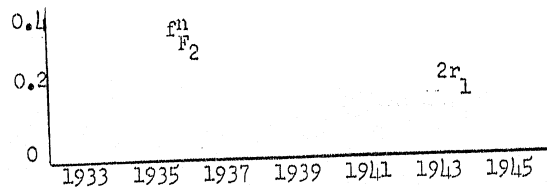$$\bar{f}_{E} = 0.345 \sin \frac{\pi}{6} \tau + 3.295$$
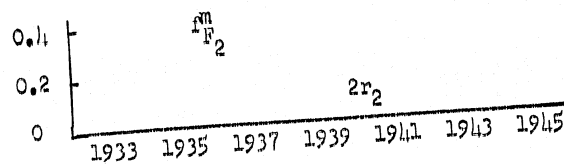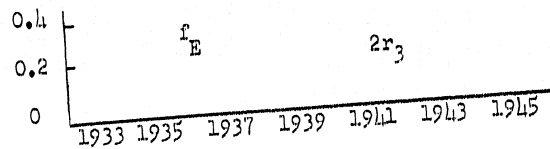

Figure 21

Figure 22

37

Figure 23

Figure 24

Here the values for the critical frequencies are expressed in megacycles. Estimation of the errors, carried out by comparison of the theoretical curves with the experimental, (Figure 19), shows the maximum deviation of the radius-vector of the curve of noon values for the F_2 layer from that obtained by calculation does not exceed 5 percent.

In the general case the following expressions may be used for forecasting purposes. In these expressions the mean annual values for the critical frequencies,

$$\overline{f}^d_{F_2W}, \quad \overline{f}^n_{F_2W}, \quad \overline{f}^m_{F_2W}, \text{ and } \overline{f}_{EW},$$

determined by the correlation equations,[1] [1. See other paper by this author in same number of this journal.] have been substituted for b, b_1, b_2, b_3 (Formulae (22) to (25)),

38

$$f_{F_2}^{d} = 2r \sin \frac{\pi}{6} t + \overline{f}_{F_2 W}^{d}, \tag{32}$$

$$f_{F_2}^{n} = 2r_1 \sin \frac{\pi}{6} t + \overline{f}_{F_2 W}^{n}, \tag{33}$$

$$f_{F_2}^{M} = 2r_2 \sin \frac{\pi}{6} t + \overline{f}_{F_2 W}^{M}, \tag{34}$$

$$f_{E} = 2r_3 \sin \frac{\pi}{6} t + \frac{6}{f_{EW}}. \tag{35}$$

The values of r, r_1, r_2 and r_3 are determined by formula (27) where there is an experimental value for the December value f_{max} or the June value f_{min}.

The character of the variation in r, r_1, r_2 and r_3 during the past cycle in the areas of their maximum values is depicted on Figures 21-24.

It may be seen from studying these diagrams that the course of the curves differ. The variation in the value $2r$ agrees with the march of the cycle; the same may be said of the variation in $2r_1$ (Figure 22) and $2r_2$ (Figure 23), but $2r_3$ varies only slightly with the development of the cycle. The more precise forecasting of the critical frequencies is limited by the inadequate accumulation of experimental data, which still requires considerable supplementation to render possible the verification and elaboration of our conclusions.

Section of scientific treatment   Received by the editors

of problems of radio technology   4 June 1947

of the Academy of Sciences USSR

BIBLIOGRAPHY

1. Chapman, S. Proc. Phys. Soc., 43, 1931.

2. Berkner, L. and Wells, H. Terr. Magn. and Atm. El. 43, No. 1
   March 1938.

3. Berkner, L. and Wells, H., Terr. Magn. and Atm. El. 39, 215 1934.

4. Appleton, E. and Naismith, R., Proc. Roy. Soc. Ser. A 150, July 1935.

5. Eccersley, T. L., Terr. Magn. and Atm. El. 45, No. 1, 1940.

6. Maeda, H., Tukada, T. and Kamochida, T. Rep. Radio Res. Japan,
   7, 109-119, 1937.

7. Arkhangel'skiy, B. F. Byulleten' ionosfernikh solnechnykh i
   geomagitnikh dannikh Soveta po radiofizika i radiotekhnike
   AN SSR (Bulletin of ionospheric, solar and terrestrial mag-
   netism data of the Council on Radio Physics and Radio Tech-
   nology of the Academy of Sciences USSR), VIII-IX, 1940.

8. Felitsyn, F. I. Astronomicheskiy Zhurnal (Astronomical Journal)
   17, 21, 1.

9. Gnevischew, M. N. and Ol, A. I., Terr. Magn. and Atm. El. 51
   No. 2, 1946.

10. Carrington, J.M.N., 19, 1, 1858.

11. Sporer, H., Publ. Astrophys. Obs. Potsdam, 11, Tafel (Table) 32,
    1881.

12. Waldmeier, M. Astronomische Mitteilungen, (Astronomical Commu-
    nication Nr. CXXXVIII, 1939.

13. Goncharov, V. L. Teoriya interpolirovaniya i priblizheniya
    funktsiy (Theory of Interpolation and Approximation of
    Functions), ONTI-GTTI, 1934.

14. Whittaker, E. (Uitteker) and Robinson, G., Matematicheskaya obrabotka
    resultatov nablyudeniy (The mathematical treatment of observational
    results). GTTI, 1933.